arXiv:nlin.CD/0211036 v1 21 Nov 2002

Chaotic Mixing in a Torus Map

Jean-Luc Thiffeault*

Department of Applied Physics and Applied Mathematics, Columbia University, New York, NY 10027

Stephen Childress†

Courant Institute of Mathematical Sciences, New York University, New York, NY 10012

(Dated: November 21, 2002)

The advection and diffusion of a passive scalar is investigated for a diffeomorphism of the 2-torus. The map is chaotic, and the limit of almost-uniform stretching is considered. This allows an analytic understanding of the transition between the superexponential and exponential phases of decay. The asymptotic state in the exponential phase is an eigenfunction of the advection–diffusion operator, in which most of the scalar variance is concentrated at small scales, even though a large scale mode sets the decay rate. The duration of the superexponential phase is proportional to the logarithm of the exponential decay rate; if the decay is slow enough then there is no superexponential phase at all.

PACS numbers: 47.52.+j, 05.45.-a

Keywords: chaotic mixing, advection–diffusion, torus maps

I. INTRODUCTION

It has recently been suggested[1] that estimates of the decay rate of the variance of a passive scalar[2–5] do not yield satisfactory results when applied to some simple maps, such as the inhomogeneous baker's map.[6,7] This also seems to be the case in laboratory experiments on periodic flows, where the decay rate is observed to be about an order of magnitude slower than the decay rate based on local arguments, such as the distribution of Lyapunov exponents.[8] The reason for this is that in chaotic advection[9] (*i.e.*, smooth flows with chaotic Lagrangian trajectories), far from the highly-turbulent regime, the presence of slowly-decaying eigenfunctions dominates the long-time decay rate.[1,10–12] This was demonstrated convincingly via a numerical approach for the inhomogeneous baker's map.[1] Here we propose to use a diffeomorphism of the 2-torus (an extension of Arnold's cat map[13]) to further investigate aspects of the decay of variance and provide some analytical results. We find that, when the map is close to uniformly stretching, the decay rate is much faster than indicated by the distribution of Lyapunov exponents, as was also found in the inhomogeneous baker's map.[1] In Fereday et al.[1] and laboratory experiments,[8], a slower decay was also observed, but far from the uniformly-stretching regime.

*Electronic address: `jeanluc@mailaps.org`

†Electronic address: `childress@cims.nyu.edu`

The paper is organized as follows. In Section II we introduce the map and derive basic expressions for the effect of advection and diffusion on a passive scalar (often referred to as temperature for concreteness). We then analyze the superexponential (Section III) and exponential (Section IV) phases of diffusion. The spectrum of variance for the exponential eigenfunction is derived in Section V, followed by a discussion of the results in Section VI.

II. ADVECTION–DIFFUSION IN A MAP

We consider a diffeomorphism of the 2-torus $\mathbb{T}^2 = [0,1]^2$,

$$\mathcal{M}(\boldsymbol{x}) = \mathbb{M}\cdot\boldsymbol{x} + \phi(\boldsymbol{x}), \tag{1}$$

where $\mathbb{M}$ is a 2×2 nonsingular matrix with integer coefficients and $\phi(\boldsymbol{x})$ is periodic in both directions with unit period. We choose $\mathbb{M}$ to have unit determinant, with an eigenvalue larger than one and the other less than one, so that even in absence of the ϕ term $\mathcal{M}$ is still chaotic. Specifically, we take

$$\mathbb{M} = \begin{pmatrix} 2 & 1 \\ 1 & 1 \end{pmatrix}; \qquad \phi(\boldsymbol{x}) = \frac{K}{2\pi}\begin{pmatrix} \sin 2\pi x_2 \\ \sin 2\pi x_2 \end{pmatrix}; \tag{2}$$

so that $\mathbb{M}$ is the Arnold cat map and ϕ is a wave term usually associated with the standard map. The map $\mathcal{M}$ is area-preserving, and for $K=0$ the stretching of phase-space elements is uniform in space; the map is always chaotic (the largest Lyapunov exponent is positive).

We consider the effect of iterating the map and applying the heat operator to a scalar distribution $\theta^{(i-1)}(\boldsymbol{x})$,

$$\theta^{(i)}(\boldsymbol{x}) = \mathcal{H}_\epsilon\,\theta^{(i-1)}(\mathcal{M}^{-1}(\boldsymbol{x})), \tag{3}$$

where ϵ is the diffusivity, and the heat operator $\mathcal{H}_\epsilon$ and kernel h_ϵ are

$$\mathcal{H}_\epsilon\theta(\boldsymbol{x}) := \int_{\mathbb{T}^2} h_\epsilon(\boldsymbol{x}-\boldsymbol{y})\theta(\boldsymbol{y})\,\mathrm{d}\boldsymbol{y}; \qquad h_\epsilon(\boldsymbol{x}) = \sum_{\boldsymbol{k}} \exp(\mathrm{i}\boldsymbol{k}\cdot\boldsymbol{x} - \boldsymbol{k}^2\epsilon). \tag{4}$$

We Fourier expand $\theta^{(i)}(\boldsymbol{x})$,

$$\theta^{(i)}(\boldsymbol{x}) = \sum_{\boldsymbol{k}} \hat{\theta}^{(i)}_{\boldsymbol{k}}\,\mathrm{e}^{\mathrm{i}\boldsymbol{k}\cdot\boldsymbol{x}} \tag{5}$$

so that (3) becomes

$$\hat{\theta}^{(i)}(\boldsymbol{x}) = \sum_{\boldsymbol{q}} \mathbb{T}_{\boldsymbol{k}\boldsymbol{q}}\,\hat{\theta}^{(i-1)}_{\boldsymbol{q}}, \tag{6}$$

with the transfer matrix,

$$\mathbb{T}_{\boldsymbol{k}\boldsymbol{q}} := \int_{\mathbb{T}^2} \exp\left(2\pi\mathrm{i}\,(\boldsymbol{q}\cdot\boldsymbol{x} - \boldsymbol{k}\cdot\mathcal{M}(\boldsymbol{x})) - \epsilon\,\boldsymbol{q}^2\right)\,\mathrm{d}\boldsymbol{x}. \tag{7}$$

For the form of the map given by (1) and (2), we have

$$\mathbb{T}_{\boldsymbol{k}\boldsymbol{q}} = \mathrm{e}^{-\epsilon\,\boldsymbol{q}^2}\,\delta_{0,Q_2}\,\mathrm{i}^{Q_1}\,J_{Q_1}\left((k_1+k_2)\,K\right), \qquad \boldsymbol{Q} := \boldsymbol{k}\cdot\mathbb{M} - \boldsymbol{q}, \tag{8}$$

where the J_Q are the Bessel functions of the first kind.

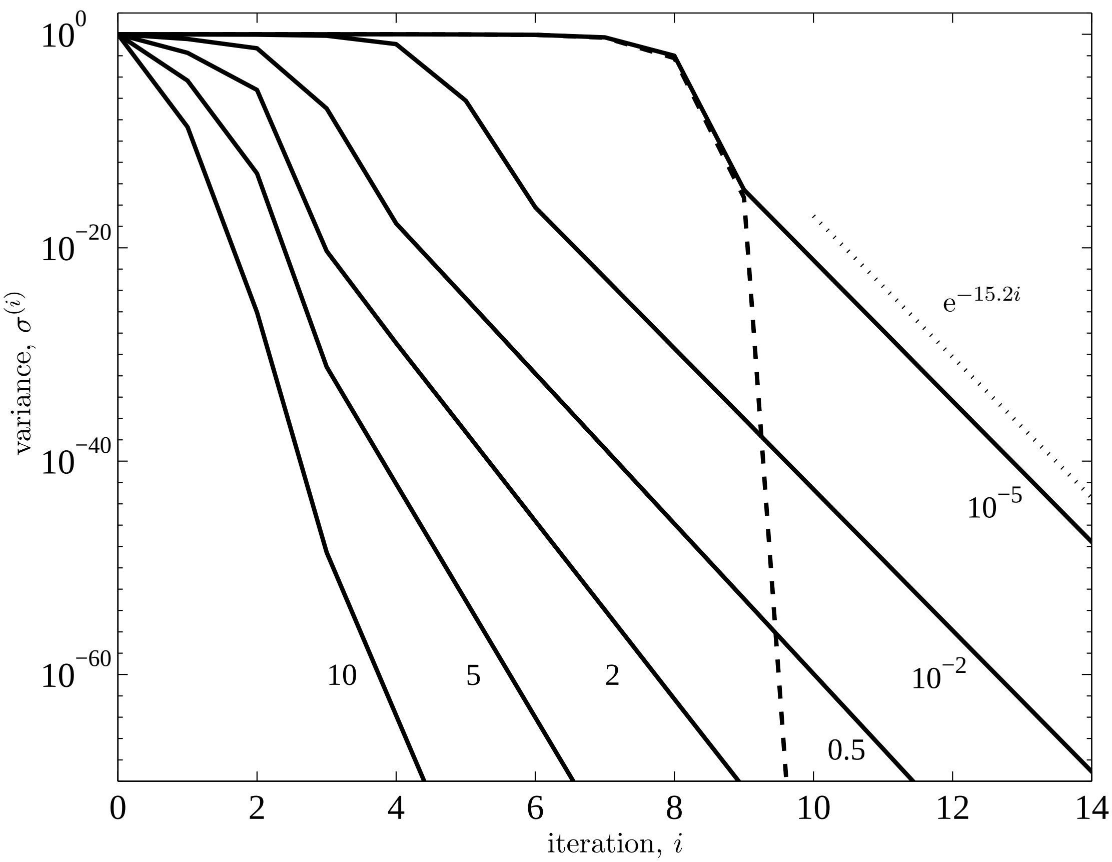

FIG. 1: Decay of total variance for varying diffusivity ϵ and $K = 10^{-3}$. The onset time of decay is logarithmic in the diffusivity, but the asymptotic exponential decay rate becomes independent of the diffusivity as $\epsilon \to 0$. The dashed curve shows the exact superexponential solution ($K = 0$) for $\epsilon = 10^{-5}$, and the dotted line is the single-mode value from Eq. (14).

In the absence of diffusion ($\epsilon = 0$), the variance

$$\sigma^{(i)} := \int_{\mathbb{T}^2} \left|\theta^{(i)}(\boldsymbol{x})\right|^2 \, \mathrm{d}\boldsymbol{x} = \sum_{\boldsymbol{k}} \sigma^{(i)}_{\boldsymbol{k}}; \qquad \sigma^{(i)}_{\boldsymbol{k}} := \left|\hat{\theta}^{(i)}_{\boldsymbol{k}}\right|^2, \tag{9}$$

is preserved by (3) (we assume the spatial mean of θ is zero), and for $\epsilon > 0$ the variance decays (Fig. 1). We consider the case $\epsilon \ll 1$, of greatest practical interest. For small K, there are three phases: (i) the variance is initially constant; (ii) it then undergoes a rapid superexponential decay; and (iii) it ultimately decays exponentially at a fixed rate, independent of ϵ, as $\epsilon \to 0$. In the first phase, the map has not yet created gradients large enough for the small diffusion to act. In the second phase, there is a rapid exponential cascade to small scales and an associated exponential diffusion, leading to a superexponential decay. As the variance is depleted by diffusion, eventually the system settles into an eigenfunction that sets the exponential decay rate in the final phase.

The existence of these three phases is well-known,[2,14] but the exponential phase is the least understood, at least for the case of smooth flows and maps. We discuss the superexponential phase briefly in Section III, and in Section IV we describe the exponential phase. We will see that if the eigenfunction of the exponential phase decays slowly enough, then there is no superexponential phase at all.

III. THE SUPEREXPONENTIAL PHASE

Initially, the variance is essentially constant because the tiny diffusivity can be neglected. However, there is a cascade of the variance to larger wavenumbers under the action of $\mathcal{M}^{-1}$ in (3). (In this phase, for small K, we can neglect the ϕ term in (1), so that the map $\mathcal{M}$ is Arnold's cat map $\mathbb{M}\cdot\boldsymbol{x}$.) This is the well-known "filamentation" effect in chaotic flows: the stretching and folding action of the flow causes rapid variation of the temperature across the folds. Thus, after a number of iterations $i_1 \simeq 1 + (\log\epsilon^{-1}/\log\Lambda^2)$,[16] where $\Lambda = (3+\sqrt{5})/2 \simeq 2.618$ is the largest eigenvalue of $\mathbb{M}^{-1}$, the diffusion can no longer be neglected. For $\epsilon = 10^{-5}$, we have $i_1 \simeq 6$ (this is always an overestimate). We now describe what happens to the variance after diffusion sets in.

For small K and $\boldsymbol{k}$, we have $J_0\left((k_1+k_2)K\right) \gg J_1\left((k_1+k_2)K\right)$, so we set $K = 0$ and retain only the $Q_1 = 0$ term in the transfer matrix (8),

$$\mathbb{T}_{\boldsymbol{kq}} = \mathrm{e}^{-\epsilon\,\boldsymbol{q}^2}\,\delta_{\boldsymbol{0},\boldsymbol{Q}} + \mathcal{O}\big((k_1+k_2)^2K^2\big)\,; \tag{10}$$

Hence, the nonvanishing matrix elements of $\mathbb{T}$ have $\boldsymbol{k} = \boldsymbol{q}\cdot\mathbb{M}^{-1}$. If initially the variance is concentrated in a single wavenumber $\boldsymbol{q}_0$ (*i.e.*, $\sigma^{(0)}_{\boldsymbol{k}} = 0$ unless $\boldsymbol{k} = \boldsymbol{q}_0$), then after one iteration it will all be in $\boldsymbol{q}_0\cdot\mathbb{M}^{-1}$, after two in $\boldsymbol{q}_0\cdot\mathbb{M}^{-2}$, etc. This amount to the length of $\boldsymbol{q}$ being multiplied by a factor $\Lambda > 1$ at each iteration. But at each iteration the variance is multiplied by the diffusive decay factor $\exp(-2\epsilon\,\boldsymbol{q}^2)$, with $\boldsymbol{q}$ getting exponentially larger. The total variance is given by

$$\sigma^{(i)} = \sigma^{(0)}\,\exp(-2\epsilon\,\|\boldsymbol{q}_0\cdot\mathbb{M}^{-(i-1)}\|^2) \simeq \sigma^{(0)}\,\exp(-2\epsilon\,\|\boldsymbol{q}_0\|^2\,\Lambda^{2(i-1)}), \tag{11}$$

so that the net decay is superexponential. The superexponential solution is represented by a dashed line in Fig. 1, with the solid line showing the numerical solution for the map $\mathcal{M}(\boldsymbol{x})$. The superexponential solution is valid until about the ninth iteration. We will revisit this breakdown of the solution in Section IV.

IV. THE EXPONENTIAL PHASE

In the superexponential phase we completely neglected the effect of the wave term in the map (1). We described the action as a perfect cascade to large wavenumbers, so that the variance was irrevocably moved to small scales and dissipated extremely rapidly. There can be no eigenfunction in such a situation, since the mode structure changes completely at each iteration. This direct cascade process dominates at first, but it is so efficient that eventually we must examine the effect of the the wave term, which is felt through the higher-order Bessel functions in the transfer matrix (8).

Consider a matrix element for which $Q_1 \neq 0$ in (8). From the definition of $\boldsymbol{Q}$, this means that the initial ($\boldsymbol{q}$) and final ($\boldsymbol{k}$) wavenumbers connected by that matrix element can differ from the condition $\boldsymbol{k}\cdot\mathbb{M} = \boldsymbol{q}$ by a factor Q_1 in their first component. Is it possible for a wavenumber to be mapped back onto itself by such a coupling? To answer this question we must seek solutions to

$$(q_1 \;\; q_2)\cdot\mathbb{M} = (q_1 + Q_1 \;\; q_2) \quad\Longrightarrow\quad (q_1 \;\; q_2) = (0 \;\; Q_1)\,. \tag{12}$$

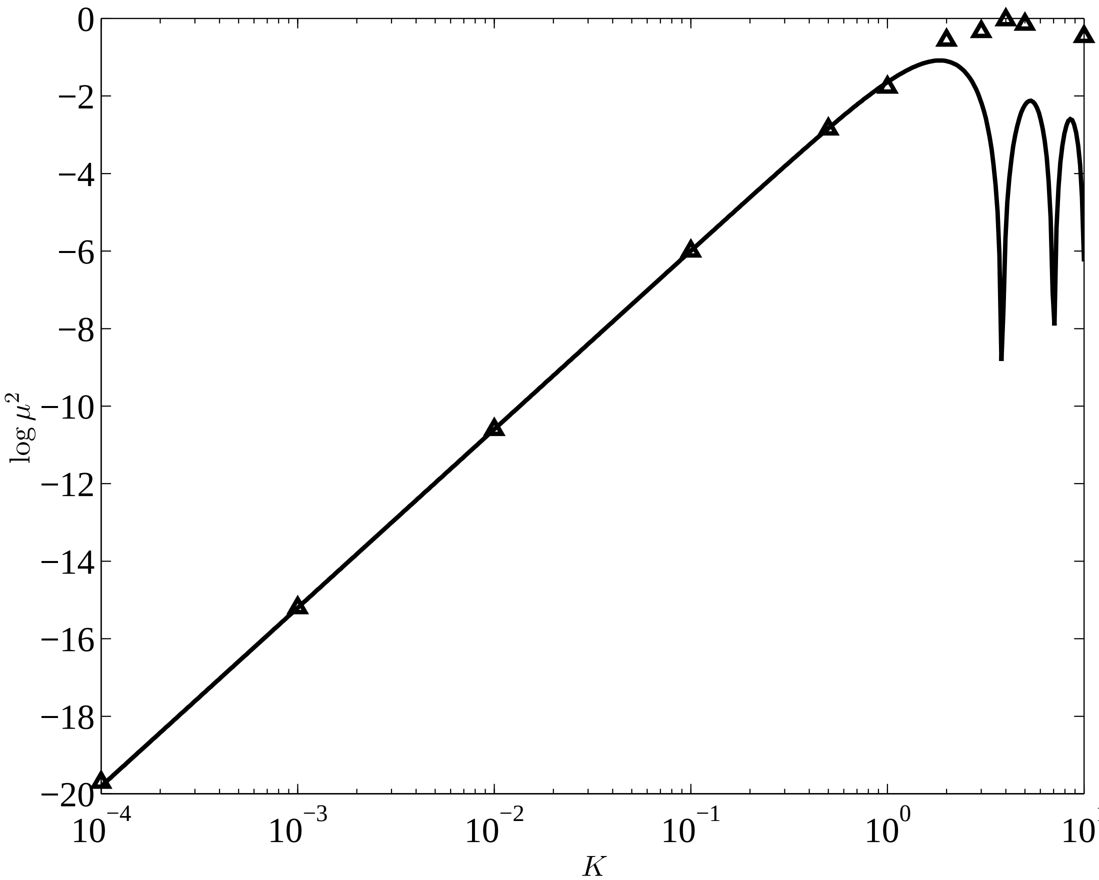

FIG. 2: Exponential decay rate $\log\mu^2$ of the variance for $\epsilon \to 0$, as a function of K and. The triangles denote numerically calculated values, and the solid line is the small-K expression (14).

So there exist modes that are mapped to themselves after one iteration: the modes that depend only on the x_2 coordinate. The matrix element connecting the $(0\ \ Q_1)$ mode to itself is

$$\mathbb{T}_{(0\ Q_1),(0\ Q_1)} = \mathrm{e}^{-\epsilon Q_1^2}\,\mathrm{i}^{Q_1}\,J_{Q_1}\left(Q_1 K\right), \tag{13}$$

which vanishes for $K = 0$, since $Q_1 \neq 0$. For small K, the dominant Bessel function is J_1, so the decay factor μ^2 for the variance is given by

$$\mu = \left|\mathbb{T}_{(0\ 1),(0\ 1)}\right| = \mathrm{e}^{-\epsilon}\,J_1\left(K\right) = \tfrac{1}{2}K + \mathcal{O}\bigl(\epsilon\,K, K^2\bigr)\,. \tag{14}$$

Hence, for small K the decay rate is limited by the $(0\ \ 1)$ mode. For $\epsilon \to 0$, the decay rate is independent of ϵ. Figure 2 shows that the single-mode decay rate agrees very well with the numerical results even for K close to unity. In the inhomogeneous baker's map the nearly-superexponential limit is for $\alpha \to 1/2$, where α is a parameter describing the inhomogeneity of the map. For that case the transfer matrix scales in a manner analogous to here as $\alpha \to 1/2$, but many more modes must be retained due to the presence of discontinuities: all the matrix coefficients decay as $(1/2)-\alpha$, with none clearly dominating. The single-mode approximation is thus far less accurate.

Now that the mechanism of exponential decay is understood (for small K), we can go back and describe the condition for breakdown of the superexponential solution discussed at the end of Section III. The superexponential decay depletes the variance very rapidly until all that is left is variance in the exponentially decaying mode $\boldsymbol{k}_0 := (0 \;\; 1)$. The superexponential phase thus ends when the variance at large wavenumbers equals that in mode $\boldsymbol{k}_0$. Assuming that the variance resides entirely in the $\boldsymbol{k}_0$ mode initially, the condition for this is

$$\mu^{i_2} = \exp(-\epsilon \, \|\boldsymbol{k}_0 \cdot \mathbb{M}^{-(i_2-1)}\|^2), \tag{15}$$

where μ is the decay factor of the variance in the $\boldsymbol{k}_0$ mode, given by Eq. (14), and the right-hand side is the superexponential solution (11). After substituting $\left\|\boldsymbol{k}_0 \cdot \mathbb{M}^{-(i_2-1)}\right\| \simeq \Lambda^{i_2-1}$, Eq. (15) must be solved numerically for i_2: for $K = 10^{-3}$ and $\epsilon = 10^{-5}$, we have $i_2 \simeq 9.2$. This is in fine agreement with the transition from superexponential to exponential in Fig. 1.

If $\epsilon \ll 1$, Eq. (15) has the approximate solution

$$i_2 \simeq 1 + \frac{\log\left(\epsilon^{-1} \log \mu^{-1}\right)}{\log \Lambda^2}, \tag{16}$$

which gives $i_2 \simeq 8$ for $K = 10^{-3}$, $\epsilon = 10^{-5}$. Subtracting $i_1 = 1 + \log \epsilon^{-1} / \log \Lambda^2$, the onset of the superexponential phase (Section III), we find that the duration of the superexponential phase is roughly

$$i_2 - i_1 \simeq \frac{\log \log \mu^{-1}}{\log \Lambda^2}, \tag{17}$$

which is independent of ϵ (at leading order), and has a weak dependence on the decay rate $\log \mu$. Unless μ is very small (recall that $0 < \mu < 1$), the superexponential phase is very short. In fact, for $\log \mu^{-1} > 1$ the decay of the $(0 \;\; 1)$ mode is slow enough that there is no superexponential phase at all, as indicated by the negative right-hand side in (17). We can thus speculate that it is unlikely that the superexponential phase can be observed in experiments, since there μ tends to be close to unity.

Note that ϵ has to be extremely small for (17) to hold: for $K = 10^{-3}$, $\epsilon = 10^{-5}$, (17) gives $i_2 - i_1 \simeq 1$, whereas the unapproximated (numerical) result is $i_2 - i_1 \simeq 2.2$. The error on (16) and (17) scales as $\log \log \epsilon^{-1}$.

V. VARIANCE SPECTRUM OF THE EIGENFUNCTION

The long-wavelength mode discussed in Section IV is the bottleneck that determines the decay rate (for small K). But this dominant mode does not determine the structure of the eigenfunction. In fact, a very small amount of the total variance actually resides in that bottleneck mode: the variance is concentrated at small scales. We now derive the variance spectrum of the eigenfunction.

The variance is taken out of the $(0 \;\; 1)$ mode in the same manner as described in Section III: there is a cascade from that mode to larger wavenumbers through the action of $\mathbb{M}^{-1}$. Neglecting the K term, the cascade proceeds from $\boldsymbol{k}_0 = (0 \;\; 1)$ as

$$(0 \;\; 1) \rightarrow (-1 \;\; 2) \rightarrow (-3 \;\; 5) \rightarrow (-8 \;\; 13) \rightarrow \ldots. \tag{18}$$

These become more and more aligned with the stable (contracting) direction of the map. The amplitude of the wavenumber is multiplied at each step by a factor $\Lambda = (3 + \sqrt{5})/2 \simeq 2.618$, the largest eigenvalue of $\mathbb{M}^{-1}$.

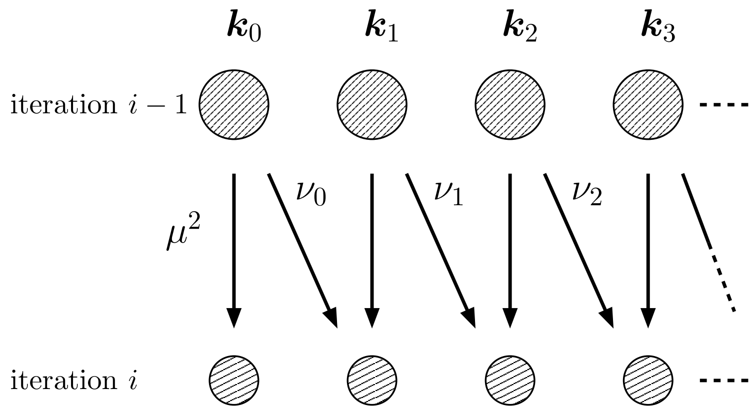

FIG. 3: Schematic representation of the cascade of variance for an eigenfunction.

The exponential decay rate suggests that the scalar concentration is in an eigenfunction of the advection–diffusion operator. Assuming this to be the case, Fig. 3 illustrates the transfer of variance between modes for an iteration of the map. At each iteration, the eigenfunction property implies that the wavenumbers are mapped back to themselves, with their variance decreased by a uniform factor $\mu^2 < 1$. This is illustrated by the vertical arrows in Fig. 3. But at the same time, because of the cascade (18), each mode is mapped to the next one down the cascade following the diagonal arrows in Fig. 3. The decrease in variance for each of the diagonal arrows is diffusive and is given by the factor $\nu_n = \exp(-2\epsilon\, \boldsymbol{k}_n^2)$. If we denote by $\sigma_{\boldsymbol{k}_n}^{(i)} := |\hat{\theta}_{\boldsymbol{k}_n}|^2$ the variance in mode $\boldsymbol{k}_n$ at the ith iteration, we have

$$\sigma_{\boldsymbol{k}_n}^{(i)} = \mu^2\, \sigma_{\boldsymbol{k}_n}^{(i-1)}, \qquad n = 0, 1, \ldots, \tag{19a}$$

$$\sigma_{\boldsymbol{k}_n}^{(i)} = \nu_{n-1}\, \sigma_{\boldsymbol{k}_{n-1}}^{(i-1)}, \qquad n = 1, 2, \ldots. \tag{19b}$$

These two recurrences can be combined to give

$$\sigma^{(i)}(\boldsymbol{k}_n) = \frac{\nu_{n-1}\,\nu_{n-2}\,\cdots\,\nu_0}{\mu^{2n}} = \mu^{-2n}\,\exp\left(-2\epsilon \sum_{m=0}^{n-1} \boldsymbol{k}_m^2\right), \tag{20}$$

where the *relative variance* in the nth mode is defined as $\sigma^{(i)}(\boldsymbol{k}_n) := \sigma_{\boldsymbol{k}_n}^{(i)}/\sigma_{\boldsymbol{k}_0}^{(i)}$. The magnitude of the wavenumber is given by the exponential recursion,

$$\|\boldsymbol{k}_n\| \simeq \Lambda\, \|\boldsymbol{k}_{n-1}\| \quad \Longrightarrow \quad \|\boldsymbol{k}_n\| \simeq \Lambda^n\, \|\boldsymbol{k}_0\| = \Lambda^n\,, \tag{21}$$

which allows us to solve for n,

$$n = \log\|\boldsymbol{k}_n\| \,/\, \log\Lambda \tag{22}$$

and rewrite (20) as

$$\sigma^{(i)}(\boldsymbol{k}_n) = \|\boldsymbol{k}_n\|^{-2\log\mu/\log\Lambda}\,\exp\left(-2\epsilon\,\boldsymbol{k}_n^2/\Lambda^2\right), \tag{23}$$

where we retained only the $\boldsymbol{k}_{n-1}^2$ term of the sum in (20) and used (21). The right-hand side of Eq. (23) for the relative variance does not (and should not if we really have an eigenfunction) depend on the iteration number, i, and depends only on n through $\boldsymbol{k}_n$. We thus let k be a continuous variable, drop i, and rewrite (23) as

$$\sigma(k) = k^{2\zeta}\,\exp\left(-2\epsilon\, k^2/\Lambda^2\right), \qquad \zeta := -\log\mu/\log\Lambda, \tag{24}$$

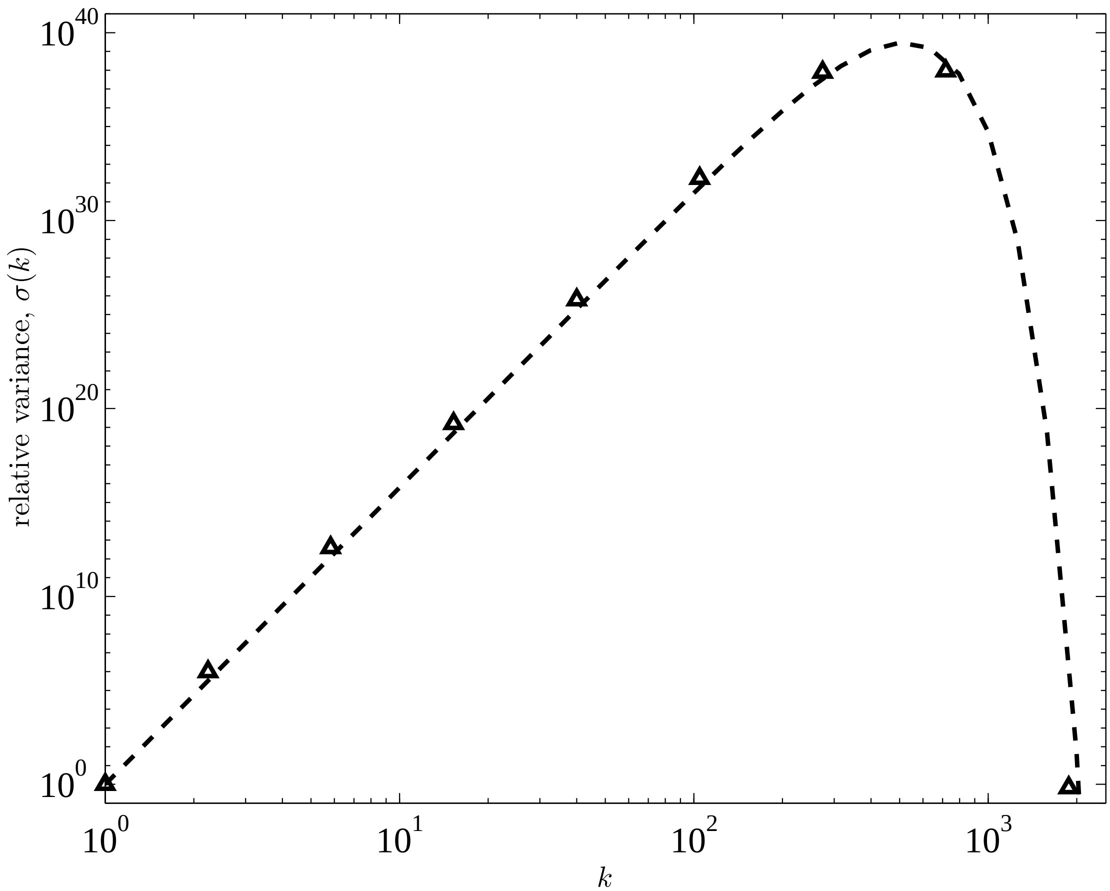

FIG. 4: Spectrum of relative variance after 12 iterations for $K = 10^{-3}$, $\epsilon = 10^{-4}$. The dashed line is the theoretical curve given by (24).

the spectrum of relative variance. The spectrum (24) is plotted in Fig. 4 and compared with numerical results for small K, showing excellent agreement. Since $\mu^2 < 1$ and $\Lambda > 1$, we conclude that $\zeta > 0$. This implies that there is more variance at the large wavenumbers than at the slowest-decaying mode $\boldsymbol{k}_0$.

To know just how much more variance, we find the maximum of (24), which is at

$$k_{\mathrm{m}} = \Lambda\,(\zeta/2\epsilon)^{1/2}, \qquad \sigma(k_{\mathrm{m}}) = k_{\mathrm{m}}^{2\zeta}\,\mathrm{e}^{-\zeta} = k_{\mathrm{m}}^{2\zeta}\,\mu^{\log\Lambda}. \tag{25}$$

The peak wavenumber thus scales as $\epsilon^{-1/2}$, the same scaling as the dissipation scale. From (25), the relative variance in that peak wavenumber scales as $\epsilon^{-\zeta}$. The wavenumber k_{m} gives an indication of the largest wavenumber that must be included in a numerical calculation to capture the decay of variance correctly. However, if the truncation size is smaller, the decay rate in the exponential phase is still captured properly, since it is determined by the $(0\ \ 1)$ mode.

VI. DISCUSSION

We summarize the three phases of chaotic mixing in smooth flows for the case of small diffusivity. In the first phase the variance is approximately conserved, and the chaotic flow (or map) creates large gradients in temperature (scalar concentration) through its stretching and folding action. This is usually called the *stirring* phase. In the second phase, the variance (that is, the squared-amplitude of each mode with the total mean subtracted) starts to decrease superexponentially, because the exponential cascade to small scales is compounded by the exponential efficiency of diffusion (Section III). This is the first of two *mixing* phases (superexponential and exponential), where diffusion plays an important role. This superexponential phase might not occur if the exponential decay rate of the slowest-decaying eigenfunction is slow enough. For very small diffusivity, the duration of the superexponential phase is independent of diffusivity.

Unless the stretching is completely uniform, the superexponential phase comes to an end because though it rapidly depletes any variance contained in the small scales, some is left behind. What is left is the eigenfunction of the advection–diffusion operator with the largest eigenvalue (all eigenvalues have modulus less than one), which then decays exponentially. The decay rate of this eigenfunction is determined by its slowest-decaying part, in the present case the $(0\ \ 1)$ mode (Section IV). The structure (spectrum) of this eigenmode is readily described as a balance between the eigenfunction property (modes are mapped to themselves with uniform amplitude) and a cascade to large wavenumbers (Section V). In the present case of a map with nearly uniform stretching, the spectrum of the eigenfunction has most of its variance concentrated at large wavenumbers, even though the small wavenumber mode $(0\ \ 1)$ dictates the rate of decay.

The decay rate of variance is outrageously fast in a map so close to being superexponential. Nevertheless, the manner in which the asymptotic regime is attained and the possibility of analytic results provide insight into the formation of the eigenfunction through the interplay of the slowest-decaying mode and the cascade to large wavenumbers. As K is made larger, the decay rates are more reasonable and a remnant of the mechanism presented here still applies.

The decay rate in the present case is completely unrelated to the Lyapunov exponent or its distribution. For small K, the distribution of the Lyapunov exponent is peaked at $\log \Lambda$ and has a very narrow standard deviation. But here the asymptotic exponential decay rate is of order $\log K$, so the decay becomes faster as $K \to 0$. This is due to the system being close to the uniform stretching (cat map) limit, which is unlikely to be the case in physical situations. Any theory based on the distribution Lyapunov exponents cannot in this case predict the decay rate, since a *global* mode dominates. For the theory of Antonsen, Jr. et al.[2], there is the further problem that, as in Fereday et al.[1], averaging over angles is not possible here, since for small K the stable manifold and the gradient of the initial condition have a nearly constant angle with respect to each other.

The large-scale eigenfunctions can lead not only to faster decay but also slower (as in Fereday et al.[1]), when compared to local, Lyapunov-exponent based approaches.[2,3] In both cases, it is the highly-ordered nature of the system (due to the large-scale, coherent nature of the flow, but also to periodic boundary conditions and walls) that gives the discrepancy. We also observe a slower decay for larger K, but no analytical theory has yet been developed to adequately describe that regime.

We observe numerically that as K is made large the spectrum of variance tends to concentrate in small wavenumbers, possibly due to the presence of a strong inverse cascade competing with the direct cascade to small scales.[15] In that limit the cascade to large wavenumbers is no longer described by the linear part $\mathbb{M}$ of the map, so there is no clear separation between the eigenfunction property and the cascade. An investigation of the decay rate and spectrum in this large K, wave-dominated limit will be the subject of future work.

Acknowledgments

The authors thank A. H. Boozer and D. Lazanja for helpful discussions. J.-L.T. was supported by the National Science Foundation and the Department of Energy under a Partnership in Basic Plasma Science grant, No. DE-FG02-97ER54441.

---

1. D. R. Fereday, P. H. Haynes, A. Wonhas, and J. C. Vassilicos, Phys. Rev. E **65**, 035301(R) (2002).
2. T. M. Antonsen, Jr., Z. Fan, E. Ott, and E. Garcia-Lopez, Phys. Fluids **8**, 3094 (1996).
3. E. Balkovsky and A. Fouxon, Phys. Rev. E **60**, 4164 (1999).
4. M. Chertkov, G. Falkovich, and I. Kolokolov, Phys. Rev. Lett. **80**, 2121 (1998).
5. D. T. Son, Phys. Rev. E **59**, R3811 (1999).
6. J. D. Farmer, E. Ott, and J. A. Yorke, Physica D **7**, 153 (1983).
7. J. M. Finn and E. Ott, Phys. Rev. Lett. **60**, 760 (1988).
8. G. Voth and J. Gollub, private communication.
9. H. Aref, J. Fluid Mech. **143**, 1 (1984).
10. D. Rothstein, E. Henry, and J. P. Gollub, Nature **401**, 770 (1999).
11. R. T. Pierrehumbert, Chaos **10**, 61 (2000).
12. R. T. Pierrehumbert, Chaos Solitons Fractals **4**, 1091 (1994).
13. V. I. Arnold, *Mathematical Methods of Classical Mechanics* (Springer-Verlag, New York, 1989), 2nd ed.
14. J.-L. Thiffeault, Phys. Lett. A (2003), in submission.
15. S. Childress and A. D. Gilbert, *Stretch, Twist, Fold: The Fast Dynamo* (Springer-Verlag, Berlin, 1995).
16. The extra 1 in i_1 appears because we diffuse at the beginning of the step in (3).